



Experimental study on dynamic characteristics and dynamic responses of accumulation slopes under frequent microseisms

Zhongping Yang^{1,2} · Xin Tian² · Yuanwen Jiang² · Xinrong Liu^{1,2} · Yuanxin Hu³ · Yunliang Lai²

Received: 2 August 2019 / Accepted: 29 July 2020 / Published online: 8 August 2020
© Saudi Society for Geosciences 2020

Abstract

Accumulation slopes are extensively distributed in the Three Gorges Reservoir area, China. The seasonal variation of reservoir's water level will induce high-frequency microseisms, which may cause landslides in reservoir banks. The study of the dynamic responses of the slope under earthquakes is the basis of the dynamic stability analysis of the slope. This paper studies the dynamic characteristics and dynamic responses of accumulation slopes under frequent microseisms by shaking table tests. Different moisture contents and dens degrees are treated as the key research contents, and a total of nine slope models have been carried out for experimental studies. The results show that the acceleration responses of the slopes under different working condition exhibit obvious "altitude effect". The dynamic characteristics refer chiefly to the inherent properties of the model, containing damping ratio and natural frequency, and the change of the latter is more sensitive. With the increasing of water content of the model, the decrease of the natural frequency is less, and the dynamic response shows a linear growth trend. The amplitude of the reduction of the natural frequency decreases with the increase of the dens degree. The results reveal the instability mechanism of the accumulation slopes under frequent microseisms and provide reference for the seismic design of the slope engineering.

Keywords Frequent microseisms · Accumulation slopes · Dynamic characteristics · Dynamic responses

Introduction

Earthquakes, as one of the most severe natural calamities in the mountainous areas, have unexpectedly caused a large number of slope stability problems, especially earthquake-induced secondary disasters, which result in massive human casualties and economic losses (Gorum et al. 2011; Tanoli et al. 2017). The Ms8.0-magnitude earthquake, happened at Wenchuan on May 12, 2008, has triggered more than 15,000

geological disasters such as landslides, collapses, and mudslides (Huang and Li 2009; Cui et al. 2011; Li et al. 2018), which directly caused 20,000 deaths (Yin 2008; Wang et al. 2014). After the earthquake, the large number of accumulation slopes caused by collapses and landslides have low safety margin. Once the stability condition is destroyed, it will bring great disaster threat to local residents. In 1985, an extremely large accumulation landslide with a volume of about 30 million cubic meters of earth and rock occurred in

Responsible Editor: Zeynal Abiddin Erguler

✉ Zhongping Yang
yang-zhp@163.com

Xin Tian
1056746300@qq.com

Yuanwen Jiang
571379270@qq.com

Xinrong Liu
liuxrong@126.com

Yuanxin Hu
270441230@qq.com

Yunliang Lai
865846819@qq.com

¹ Ministry of Education, Key Laboratory of New Technology for Construction of Cities in Mountain Area, Chongqing University, Chongqing 400030, China

² School of Civil Engineering, Chongqing University, Chongqing 400045, China

³ Extension Project Headquarters Chongqing Airport Group Co. Ltd., Chongqing 401120, China

Xintan town, Hubei Province, destroying 1569 houses, 64 wooden ships, and 13 motor boats, resulting in the death of 10 shipmen and the forced suspension of navigation for 12 days (Huang et al. 2009). In 2014, a large amount of gravel and mud poured into a village after a massive landslide in Badakhshan Province, Afghanistan, causing more than 2100 deaths and 2000 missing (Zhang et al. 2015). The Three Gorges reservoir area has also been a region with serious geologic hazards from time immemorial (Zhang et al. 2012; Wang et al. 2015); a total of about 2000 landslides have been discovered, of which accumulation slopes account for 64% (He et al. 2007; Guo et al. 2017). Since the impounding in 2010, the earthquake frequency in the Three Gorges Reservoir area has increased significantly (Liu et al. 2009; Liu et al. 2012a). According to statistics data, the earthquake frequency of being 541 that occurred in 2003 is 10 times larger than that in 1996–2002. The earthquake frequency in 2004 is 1062, twice as many as that in 2003, and the intensity has also increased, with magnitude generally under Ms. 4.0. Since 2008, the induced earthquakes have always been of high frequency, which has been characterized by small magnitude, shallow hypocenter, and fast energy attenuation (Li and Huang 2008). Although the reservoir-induced earthquake has a small magnitude, the focal depth is very shallow, which makes the energy release relatively concentrated. The site intensity of actual induced local earthquake is much larger than that of tectonic earthquake with same magnitude. Thus, the problem of seismic stability of accumulation slopes has also become increasingly prominent.

At present, from the perspective of the theory of fundamental mechanics, the evaluation of slope stability under static load has become gradually mature, but the dynamic characteristics and dynamic responses of slopes under dynamic loads need to be deeply discussed. Compared with the change of external factors, such as human engineering activities, rainfall, and so on which induce landslides, the dynamic responses of slopes under earthquakes are much more complicated (Zhou et al. 2013; Tang et al. 2015). Vibration table tests and centrifuge model tests are commonly employed to investigate the dynamic characteristics and dynamic responses of slopes. However, most of the vibration table tests that have been conducted are based on soil and rock slopes (Wartman et al. 2005; Wang and Lin 2011); few involves accumulation slopes. And most of the research is limited to the dynamic responses and dynamic characteristics of slopes under seismic waves with different seismic parameters (such as frequency, type, amplitude, etc.) (Xu et al. 2008), but without considering the influence of the characteristics of the slope itself (e.g., water content of slope, compactness of slope, etc.).

Accumulation slope refers to the special geological body composed of Quaternary deposits or sediments on the earth surface. The geological conditions of the Three Gorges Reservoir area are complex, and a large number of

accumulations are distributed near the river valley, which are not only large in scale, various in types, complex in origin, but also frequently cause geological disasters, so they deserve attention. Accumulation slope is characterized by loose structure, low safety margin, and wide distribution, sudden, and strong hazards (Jiang 2012a). Among the accumulation slopes in the Three Gorges Reservoir area, 30.1% are in the basic stable state and 69.9% are in the potential unstable state (Tang 2013). The repeated action of the earthquake will cause the physical and mechanical parameters of the accumulation slope to decrease continuously, and its stability will become worse and worse. The previous research results mainly involved the behavior of the slope in the critical unstable state or under the strong earthquake (Tao et al. 2014; Massey et al. 2017), but little attention is paid to the effect of frequent microseisms on the long-term stability of the accumulation slope. Microseisms are successive vibrations of the land surface caused by rock failure or fluid disturbance, constituting the normal background oscillations of seismograms (Donn 1966). Therefore, the effects of frequent microseisms on the dynamic characteristic and dynamic response of accumulation slopes are worthy of attention. At present, there are few research achievements on dynamic characteristics and dynamic responses of accumulation slopes, so it is necessary to study the long-term stability of the accumulation slopes under the action of frequent microseisms. It has important engineering reference value for the development of reasonable geological disaster prevention and control schemes in the reservoir area and the reduction of the damage that geological disasters may cause to people's lives and property.

The aim of this paper is to research the dynamic characteristics and dynamic responses of accumulation slopes with different slope structure, slope moisture content, and compactness under the frequent microseisms through the model test and theoretical analysis of the laboratory shaking table tests, and the relevant conclusions have important reference significance for further reservoir construction and its prevention, as well as the control of the geological disaster in the reservoir area.

Experimental design of shaking table model

Similarity relation design

In present study, the model slopes without archetype geometry size simulate the accumulation slopes in the reservoir area. Nevertheless, to simulate larger prototype slopes, bigger geometric similarity coefficients should be obtained as much as possible. According to the bearing capacity and technical parameters of the shaking table and the boundary condition of the models (Ye et al. 2012; Yang et al. 2013), this experiment takes the length of the model, the mass density, and the acceleration as the control variables and derives the similarity

relation between the physical quantities according to the similarity theorem (Brand 1957; Wu et al. 2007). The main similarity coefficients of the model, which are the ratios of the corresponding physical parameters of the prototype to those of the model, are shown in Table 1.

Materials

The similarity relation between the model and the prototype is realized by the characteristics of similar materials. It is of great consequence that the selection of similar materials and the determination of the related parameters, which is related to the available value of the experimental data. After comprehensively considering a variety of materials, six types of materials, including barite powder, quartz sand, gypsum, gypsum retarder, water, and glycerin, were selected as the similar materials for the model bedrock. Among them, barite powder and quartz sand play the role of fine aggregate and coarse aggregate, respectively; gypsum and water play a cementing role after mixing; glycerin takes the role of water retention, and gypsum retarder can delay the initial setting time of gypsum, ensuring the construction time of the slope model.

The accumulation body of this experiment is taken from the accumulation slope of the Three Gorges Reservoir area, which is a mixture of clay, sandstone, and mudstone. The gravel is mainly composed of sandstone and mudstone, with large mudstone content. The model of the accumulation body is a combination of soil and rock, which usually distinguishes “soil” and “stone” according to the particle size. Currently, the universal threshold of soil and stone is 5 mm (Jia et al. 2010; Shu et al. 2012). “Stone” is defined as the grain size larger than 5 mm, while the “soil” is defined as less than 5 mm. At the same time, the size of particle should meet the condition of size similarity ratio, so the threshold of soil and stone is fixed as 2 mm in this test. And the samples with the particle size below 20 mm are selected to rematch the soil, based on the new gradation after the conversion of the original gradation of the soil samples consistent with the similarity ratio.

After retrieving the soil samples, two groups of soil samples with 100 kg were weighed, and they were dried for 24 h under the condition of 105 C and screened. Then, the water content, the dry density, the void ratio, the stone content, and the average particle gradation were determined. It can be seen from the screening results (Fig. 1a) that the effective diameter of the original soil samples is 0.45 mm, the constrained grain size is 9.68 mm, the median diameter is 2.98 mm, the non-uniform coefficient is 20.58, the curvature coefficient is 1.95. The dry density of the soil samples is 1921 kg/m³, the natural water content is 4.11%, and the void ratio is 0.35. 5 mm as a threshold standard was taken to distinguish the soil and the stone. Therefore, the stone content is 56.7%, of which the sandstone content is about 16.2% and the mudstone content is about 40.5%.

The original soil samples were artificially hammered and sieved for obtaining the new ones, and they were redistributed according to the new grading curve (Fig. 1b). With the earth-rock threshold of 2 mm as the standard, the stone content of the reconstituted soil is about 55%, of which the sandstone content is about 15% and the mudstone content is 40%. The screening results show that the effective diameter of the reconstituted soil is 0.07 mm, the constrained grain size is 5.5 mm, the median diameter is 1.2 mm, the non-uniform coefficient is 78.57, and the curvature coefficient is 2.74. Moreover, the void ratio of the reformulated soil samples is 0.36, almost like that of the original soil samples.

Slope model construction

There are 44.9% of the accumulation slopes in the Three Gorges Reservoir area with the slope angle of 20°~30°, and the slopes with slope angle of 40°~50° only account for 2.5% (Tang 2013); thus, lots of studies (Zhou et al. 2009; Chen 2016) related to the slope with slope angle of 20°~30° have been conducted. However, some researches (He et al. 2010; Chen 2015) show that the slope angle has significant effects on the velocity amplification coefficient, the displacement

Table 1 Similarity factor of key physical parameters in model test

Physical quantity	Similarity coefficient	Physical quantity	Similarity coefficient
Internal friction angle	$C_\psi = 1$	Earthquake acceleration	$C_a = 1$
Elastic modulus	$C_E = C_\rho C_L = 22.8$	Acceleration of gravity	$C_g = C_a = 1$
Area	$C_S = C_L^2 = 520$	Velocity	$C_v = (C_L C_a)^{1/2} = 4.8$
Quality	$C_M = C_\rho C_L^3 = 11,852$	Linear displacement	$C_u = C_L = 22.8$
Bulk density	1	Force	$C_F = C_\rho C_L^3 C_a = 11,852$
Density	$C_\rho = 1$	Strain	$C_\epsilon = C_\rho C_L C_a / C_E = 0.7$
Cohesion	$C_c = C_\rho C_L C_a = 22.8$	Stress	$C_\sigma = C_\rho C_L C_a = 22.8$
Poisson ratio	$C_\mu = 1$	Frequency	$C_f = (C_a / C_L)^{1/2} = 0.21$
Geometry size	$C_L = 22.8$	Time	$C_t = (C_L / C_a)^{1/2} = 4.8$
Acceleration	$C_A = C_a = 1$	Damping ratio	$C_\xi = 1$

Cities in Mountain Area (Chongqing University). The shaking table testing system is produced by the ANCO company in the United States, and the hardware of ANCO vibrator mainly including computer, countertop, actuator, hydraulic power supply, control cabinet, and so on. The primary technical parameters were 1.2 m × 1.2 m of table size; 0–50 Hz of frequency; 1 T of maximum model weight; ± 100 mm of maximum horizontal displacement; ± 1.2 g (1000 kg) of maximum horizontal and vertical accelerations.

Loading scheme

To study the dynamic characteristics and dynamic responses of the accumulation slopes, the white noise, natural wave, and artificial wave were applied as earthquake waves in the test. The natural wave was obtained from the Ms 5.1-magnitude earthquake that occurred at 13:04 on December 16, 2013, in the Badong County in China. The focal depth of this earthquake is approximately 5 km, and the duration is about 7 s, which is consistent with the characteristics of reservoir-induced earthquakes (Tao 2006). The magnitude of reservoir-induced earthquakes is small, generally below level 4. Most of them are microseisms, and the focal depth is extremely shallow (mostly in the range of 3–5 km). Compared with the tectonic earthquakes, the reservoir-induced earthquakes have a higher shaking frequency and epicentral intensity, and the energy decays more quickly. The peak amplitude of the natural wave is scaled to four grades: 0.04 g, 0.06 g, 0.09 g, 0.15 g. The artificial wave is sine wave of different frequencies and amplitudes, it holds the same time as the natural wave (7 s), and its peak amplitude grade is 0.04 g, 0.15 g, 0.2 g, 0.4 g and frequency class is 5 Hz, 10 Hz, 15 Hz, 30 Hz. Firstly, the measured seismic wave is compressed according to the time scaling factor, and then, the amplitude of the measured wave is scaled along the whole time axis to obtain the input wave amplitude of the test. The shaking table test is a plane strain problem, so the horizontal one-way vibration is selected as the vibration direction, which is consistent with the slope inclination.

A number of studies have confirmed that the reservoir-induced earthquakes are continuous and can occur 2–4 times in 1–3 days (Suzanne 2003; Wang 2004). Due to the similar magnitude and intensity, the reservoir-induced earthquakes are difficult to be divided into foreshock, main shock, and aftershock, so it is more appropriate to take them as a sequence. Because of these features, the natural seismic wave utilized actually in the shaking table test was preprocessed (Jiang 2012b; Liu et al. 2018): four natural waves of about 7 s (the main shock section) were spliced together as a complete sequence of earthquake wave and then compressed on the basis of the time similarity coefficient ($C_t = 4$).

The amplitude and frequency of the input wave, the loading scheme for this test is shown in Table 2. The first 12

loading conditions are mainly used to analyze the basic characteristics of the dynamic responses. The 500 microseisms (0.04 g natural waves) and the 500 small earthquakes (0.15 g sine waves) are mainly used to study the variation law of the dynamic characteristic parameters with different times of earthquake action. The reservoir-induced earthquakes are characterized by the fact that multiple earthquakes of the same magnitude may occur consecutively in a short time. From 1959 to 2007, more than 5000 earthquakes with the magnitude of 1 or so have been monitored in the Three Gorges Reservoir area (Zhao 2009). In the vibration table test, an input wave used for excitation model is referred to as a working condition. After each excitation working condition is applied, the loading is stopped for observing and recording the model after vibration, and then, the next working condition is applied. Thus, the paper applies 50 times of (2 min apart) natural waves to the model to simulate the damage caused by frequent microseisms on the accumulation slope. In order to obtain the dynamic characteristic parameters, the slope model is scanned by white noise after every 50 times of seismic loading or there is significant damage.

Dynamic response analysis

The dynamic response of the accumulation slope under the dynamic load is related to the rock and soil mechanics parameters, the dynamic load parameters of the slope, the slope's geometry and material impedance contrasts (Massey et al. 2017; Yang et al. 2018), and the acceleration is an undoubtedly convenient and intuitive index for analyzing the dynamic response (Yang et al. 2005; Srilatha et al. 2013). The measuring instruments are the accelerometers of type 173A500 and charge sensitivity of 25 pC/g arranged in the model. The acceleration data is analyzed and the influence of the dynamic load, the structure of the slope, the water content, and the density on the dynamic response are also studied. And the acceleration amplification factor is used to depict the dynamic response of the model. In order to uniformly depict the acceleration response law of the model, the amplification coefficient of peak ground acceleration (PGA), which defined as the ratio of the acceleration response peak of each measuring point and the peak value of the measuring acceleration of the tabletop, is selected as the analysis index.

Frequency effect

Figure 3 shows the varieties of PGA amplification factor of different models under 0.04 g sine wave with different frequency (5–30 Hz). The results show that the PGA amplification factor increases with the elevation in all models under all conditions, which is consistent with the rock slope (Fan et al. 2016; Feng et al. 2018). With the increase of frequency, the

Table 2 Loading plan of shaking table test

Condition	Amplitude/ g	Wave type (<i>X</i> -direction)	Duration time/s	Frequency/Hz	Loading times
1	0.08	White noise 1	30		1
2	0.04	Sine wave	7	30	1
3	0.04	Natural wave	7	32	1
4	0.04	Sine wave	7	5	1
5	0.04	Sine wave	7	10	1
6	0.04	Sine wave	7	15	1
7	0.04	Sine wave	7	30	1
8	0.04	Natural wave	7	32	1
9	0.06	Natural wave	7	32	1
10	0.09	Natural wave	7	32	1
11	0.15	Natural wave	7	32	1
12	0.08	White noise 2	30		1
13–62	0.04	Natural wave	7	32	50/every 2 min
63	0.08	White noise 3	30		1
Repeat 13–63 loading conditions until the action of 500 microseisms					
525–574	0.15	Natural wave	7	32	50/every 2 min
575	0.08	White noise 3	30		1
Repeat 525–575 loading conditions until the action of 500 microseisms					

variation range of PGA amplification factor under high-frequency conditions is greater than the low-frequency conditions in the same model. As shown in Table 3, the higher-frequency input motions (30 Hz) are similar to the natural frequency of the model slope. Therefore, the effects of amplification are likely to be larger when excited by earthquakes with predominant frequencies similar to the fundamental frequency of the slope.

For the models with different moisture contents (Fig. 3a, b, c), the variation range of PGA amplification factor under

high-frequency conditions is greater than that under low-frequency conditions, and this trend continuously enhances with the increase of moisture content.

For the models with different dry densities (Fig. 3d, e, f), the variation range of PGA amplification coefficient of the model with low dry density is larger than that with high dry density at 30 Hz. Actually, at this condition, the variation range of PGA amplification factor of the model with dry density of 1700 kg/m³ increases by 29.7% compared with the model with dry density of 2100 kg/m³, and the amplification

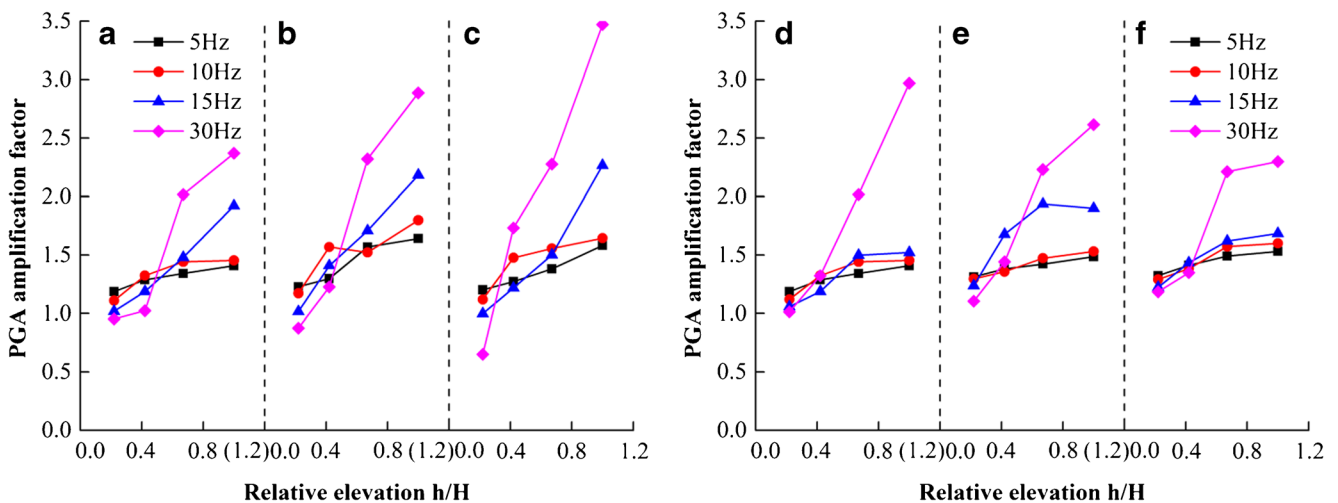


Fig. 3 PGA amplification factor of models under seismic waves with different frequency. **a** Model with moisture content of 4%. **b** Model with moisture content of 7%. **c** Model with moisture content of 10%. **d**

Model with dry density of 1700 kg/m³. **e** Model with dry density of 1900 kg/m³. **f** Model with dry density of 2100 kg/m³

Table 3 Natural frequency and damping ratio of the model

Sequence number of white noise	Natural frequency	Damping ratio	Sequence number of white noise	Natural frequency	Damping ratio
WN1	39.3969	0.1080	WN11	34.3037	0.1162
WN2	37.8976	0.1013	WN12	31.1288	0.1319
WN3	39.9969	0.0916	WN13	28.8602	0.1739
WN4	36.8596	0.0962	WN14	30.2478	0.1560
WN5	40.3875	0.0911	WN15	28.3103	0.2063
WN6	36.7784	0.1222	WN16	29.2790	0.1646
WN7	33.2911	0.1181	WN17	29.1727	0.1863
WN8	34.3100	0.1297	WN18	30.4976	0.2087
WN9	33.0599	0.1123	WN19	29.8414	0.2134
WN10	33.1287	0.1455	WN20	30.3570	0.2278

factor is remarkable. While this phenomenon is not distinct at 5 or 10 Hz, the maximum variation is found at intermediate density (1900 kg/m³) at 15 Hz.

Amplitude effect

Figure 4 shows the varieties of PGA amplification factor of different models under natural wave with different wave amplitude (0.04 g, 0.06 g, 0.09 g, 0.15 g). The results show that the PGA amplification factor of all models decreases with the increase of the amplitude of the loading wave, and the reduction at the slope shoulder (the point with the highest elevation) is greater than that at slope foot (the point with the lowest elevation).

Compared with the variety curves of the models with different moisture contents (Fig. 4a, b, c), the PGA amplification factor is increasing gradually with the increase of moisture content.

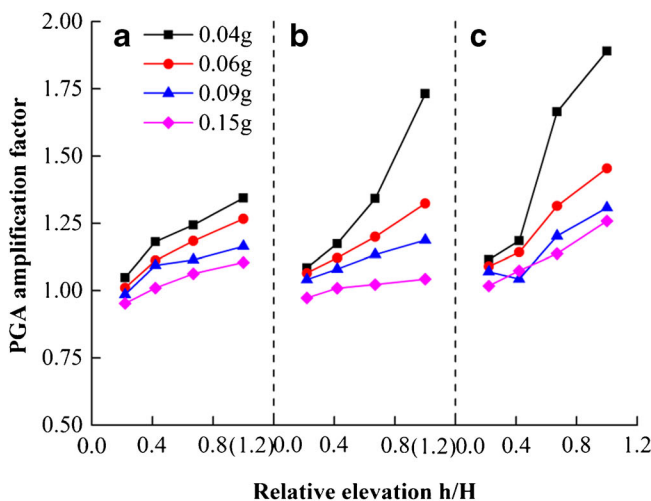
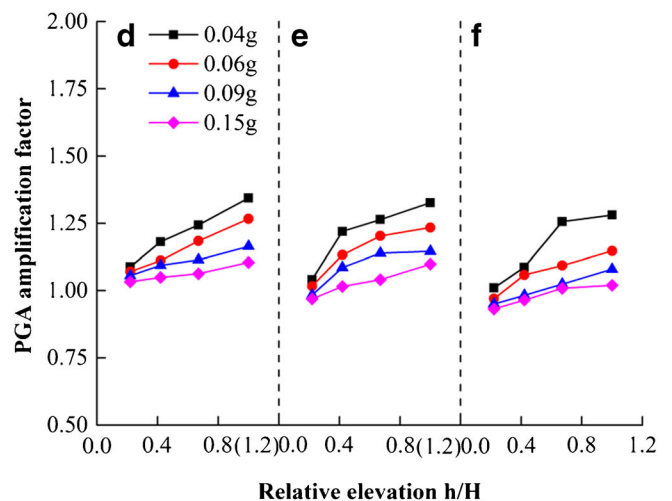


Fig. 4 PGA amplification factor of models under seismic waves with different amplitude. **a** Model with moisture content of 4%. **b** Model with moisture content of 7%. **c** Model with moisture content of 10%. **d**

Compared with the variety curves of the models with different dry densities (Fig. 4d, e, f), the greater the dry density is, the larger the variation of PGA amplification factor at the same height of the slope surface is, and the PGA amplification factor is increasing gradually with the increase of dry density.

Dynamic characteristic analysis

The dynamic response of the slope is closely related to the dynamic characteristic, which is the internal cause of the dynamic response. As the natural frequency and damping ratio are closely related to the damage degree of slope, the paper chooses them to reflect the dynamic characteristics. After stimulating the model by white noise, the acceleration time history curves of all measurement points are obtained, and then the transfer function is inversely calculated, and the dynamic characteristic parameters can be obtained by combining the transfer function curve. According to the data analysis



d Model with dry density of 1700 kg/m³. **e** Model with dry density of 1900 kg/m³. **f** Model with dry density of 2100 kg/m³

software of MATLAB and Microsoft Excel, the transfer function method (Eduard 2000; Duarte and José 2011) is utilized to obtain the dynamic characteristic parameters of slope (natural frequency and damping ratio), as presented in the Formula (1).

$$T_{xy}(f) = P_{yx}(f)/P_{xx}(f) \quad (1)$$

where $T_{xy}(f)$ is the transfer function of the input signal (x) of the measurement point on the table and the output signal (y) of the measurement point inside slope, $P_{yx}(f)$ is the cross-power density spectrum function between the input signal and the output signal, $P_{xx}(f)$ is the self-power density spectrum function of the input signal, and f is the signal frequency.

Taking the model with moisture content of 7% and dry density of 1900 kg/m^3 as an example, its natural frequency and damping ratio are shown in Table 3. To observe the trend of the natural frequency and damping ratio more intuitively, the curve in the loading process is shown in Fig. 5. The results show that, as the loading process is carried out, the natural frequency of the model generally presents a downward trend, with a decrease of 22.9%; the damping ratio shows an upward trend with an increase of 110.9%. Due to the internal crack propagation, the macro-mechanical properties of the accumulation slope under frequent microseisms deteriorate. Each time the earthquake acts, the slope will suffer a certain amount of damage, which will continue to accumulate until the failure occurs. In the *OA* section (the initial stage of the test), the natural frequency exhibits a weak upward trend with the maximum increase of 2.5%; the damping ratio exhibits a weak downward trend with a decrease of 15.6%. This result is due to the fact that vibration intensity is low in the early stage of the test, the slope model is more compact after shaking, and the dynamic load enhances the stability of the model. In the *AB* section (the middle stage of the test), the natural frequency decreases gradually in the form of leaping, with a decrease of 29.9%; the damping ratio increases in the form of leaping, with an increase of 126.5%. Obviously, the model damage

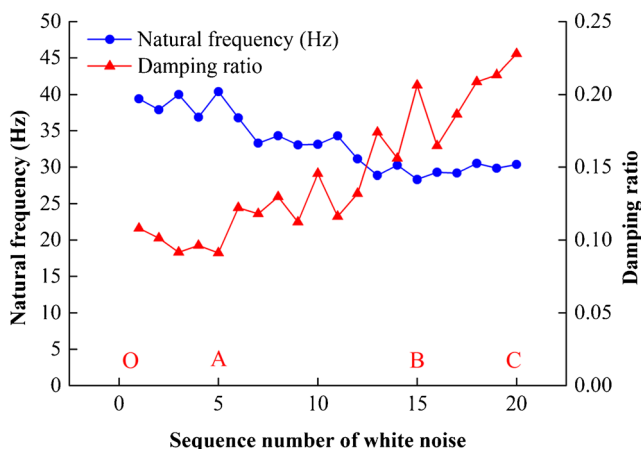


Fig. 5 The curves of the natural frequency and damping ratio of model

gradually increases and the shear modulus decreases with the loading. The damping ratio and natural frequency, which reflect the dynamic characteristics of the model, are changing significantly. The repeated cycles of the dynamic load make the state of the accumulations cyclically change between loose and compact. Therefore, the load of a certain adjacent stage shows a leaping trend, while the overall trend remains unchanged. In the *BC* section (the final stage of the test), when the weak part of the slope is deformed and destroyed under the action of seismic waves, the remaining part of the model re-enters into a new relatively stable stage. This part will only undergo a new deformation and damage when the number of loadings is more or the intensity of seismic waves is greater. The transfer function curve needs smooth processing when solving dynamic characteristic parameters through the transfer function, which will reduce the accuracy of the damping ratio; so, the variation curve of the damping ratio fluctuates greatly. At this moment, the displacement of the accumulations temporarily stops increasing.

The influence of moisture content on the dynamic characteristics

Taking the three models with dry density of 2100 kg/m^3 (moisture content of 4%, 7%, and 10%, respectively) as an example, which are shown in Fig. 6, the effect of water content on the dynamic characteristics is analyzed. In the initial period, the natural frequency of the model with low water content (4%) is obviously higher than that with high water content (10%), and the former is 12.2% higher than the latter. By contrast, the damping ratio of the former is 27.4% lower than that of the latter. It indicates that the moisture content is unfavorable to the dynamic characteristics of the model.

In the early period of vibration compaction, the higher the water content is, the smaller the degree of vibration compaction of the model is. In the stage of the damage development, the natural frequency of the model with low water content

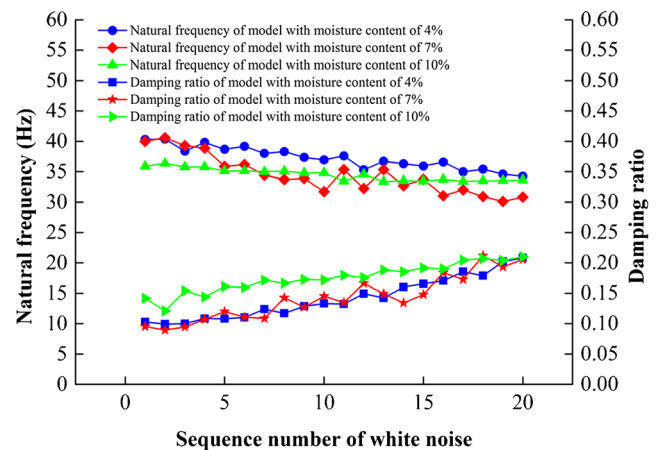


Fig. 6 The curves of natural frequency and damping ratio of the model with different moisture content (the dry density = 2100 kg/m^3)

decreases by 8.1% and the damping ratio increases by 68.7%. Nevertheless, the natural frequency of the model with high moisture content decreases by 13.3%, and the damping ratio increases by 86.4%. It shows that reducing the moisture content is beneficial to mitigate the development of damage and variation rate of the dynamic characteristics, contributing to the dynamic stability of the model.

In the process of the damage development, although the variation trends of the models with different water contents are different, as the damage of a certain energy level of vibration develops to the end, the difference in dynamic characteristics among the models with different moisture contents is getting smaller and smaller, indicating that the difference of moisture contents has no obvious effect on the residual strength of the models.

The influence of dry density on the dynamic characteristics

Taking the three models with water content of 4% (dry density of 1700 kg/m^3 , 1900 kg/m^3 , 2100 kg/m^3) as an example, which are shown in Fig. 7, the effect of dry density on the dynamic characteristics is analyzed. Before the application of dynamic load, the dry density has a significant influence on the initial natural frequency of the model but no obvious effect on the damping ratio. This phenomenon shows that the change of the natural frequency is more sensitive than that of the damping ratio, and it is more convincing to use it as an index for judging the damage degree of the model. In addition, the greater the dry density is, the less damage the model has.

In the stage of vibration compaction, the natural frequency of the model with dry density of 1700 kg/m^3 increases by 5.7% while the damping ratio decreases by 9.3%. However, the natural frequency of the model with dry density of 2100 kg/m^3 increases by 0.17% and the damping ratio decreases by 3.5%. It is because the model with small dry density is more loose, and it is easier to compact under the action

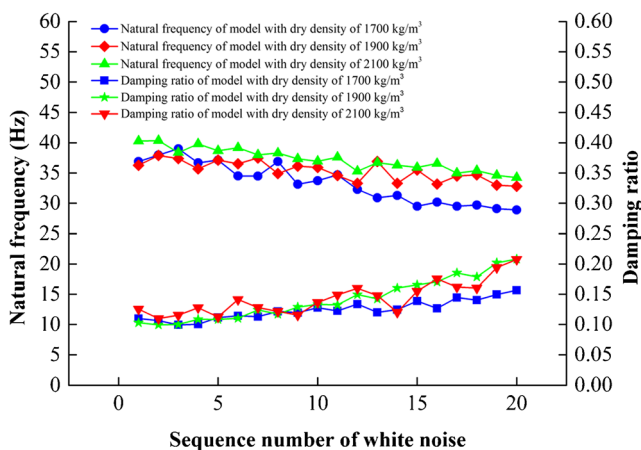


Fig. 7 The curves of natural frequency and damping ratio of the model with different dry density (the moisture content = 4%)

of the initial low-intensity vibration load compared with the model with large dry density.

With the increase of the vibration times, the model entered the cumulative stage of damage. In terms of the natural frequency, the model with small dry density has a larger reduction and faster damage development. Additionally, the model with large dry density increases more and the damage develops faster from the aspect of damping ratio. Since the natural frequency is more suitable than the damping ratio as an index of the model damage, the smaller the dry density is, the faster the damage of the model will develop.

With the application of the dynamic load close to the end, the natural frequency of the model with dry density of 1700 kg/m^3 is 18.5% lower than that with dry density of 2100 kg/m^3 , while the damping ratio is 33.1% lower. The evaluation index is based on the natural frequency, so the damage of the model with small dry density is lower than that with large dry density at the end of the loading. And the variation between them is large, indicating that the difference of the dry density has a significant influence on the residual strength of the model. In addition, as the dry density increases, the effect of the difference in dry density on the residual strength of the model gradually weakens.

Conclusions

Based on the design of the similar relationships, the selection of the similar materials and the design of the shaking table model test, which is carried out on the slope models with different moisture contents and dry densities, the main conclusions are as follows.

1. The acceleration responses of slopes under different conditions exhibit “elevation effect”. The elevation effect embodied the vertical amplification of acceleration response, that is, the greater the elevation is, the stronger the response is.
2. Under the action of different frequency conditions, the variation range of PGA amplification factor under high-frequency conditions is greater than the low-frequency conditions, and the greater the frequency and water content are, the smaller the dry density is, the more obvious the phenomenon is.
3. Under the conditions of different acceleration amplitudes, the PGA amplification factors of all models decrease with the increase of the amplitude of the loading waves, the reduction at the shoulder position is greater than that at the slope foot, and the greater the moisture content and dry density are, the more obvious the phenomenon is. This result is almost the same as that in the soil slope (Xu et al. 2008) and rock slope (Liu et al. 2012b).

4. The natural frequency is more sensitive than the damping ratio for the parameters representing the dynamic characteristics. The reduction of water content is beneficial to slow down the change rate of dynamic characteristics and is conducive to the dynamic stability of the model, while the moisture content has little effect on the residual strength of the model. The smaller the dry density is, the faster the damage develops; and the greater the dry density is, the less impact the dry density on the residual strength of the model has.

This paper has revealed the dynamic responses and dynamic characteristics of accumulation slopes under frequent microseisms. In further researches, the numerical simulation will be applied to study the effect of reservoir water level on the stability of accumulation slopes and the failure modes.

Acknowledgments The authors would like to thank the editors and the anonymous reviewers for their helpful and constructive comments. The authors thank greatly to masters Wankun Li, Denghua Li from Chongqing University for their helps during the experiment.

Funding information This work was supported by the National Natural Science Foundation of China (Grant No. 41772306), the National Key R&D Program of China (Grant No.2018YFC1504802), and the Fundamental Research Funds for the Central Universities (Project No. 2019CDCG0013).

References

- Brand L (1957) The Pi theorem of dimensional analysis. *Arch Ration Mech Anal* 1(1):35–45
- Chen WQ (2015) The stability analysis of thick accumulation slope in the three gorges reservoir area under the action of frequent microseism. Chongqing University, Chongqing
- Chen WG (2016) Study on evaluation parameters and prediction method based on coupling of hydrodynamic and displacement of debris landslide—taking typical debris landslide in three gorges reservoir area as an example. Qingdao University of Technology, Qingdao
- Cui P, Chen XQ, Zhu YY, Su FH, Wei FQ, Han YS, Liu HJ, Zhuang JQ (2011) The Wenchuan earthquake (may 12, 2008), Sichuan Province, China, and resulting geohazards. *Nat Hazards* 56(1): 19–36
- Duarte V, José SC (2011) Identifying digital and fractional transfer functions from a frequency response. *Int J Control* 3:445–457
- Eduard E (2000) The slope of a transfer function. *Int J Control* 13: 1249–1254
- Fan G, Zhang JJ, Wu JB, Yan KM (2016) Dynamic response and dynamic failure mode of a weak intercalated rock slope using a shaking table. *Rock Mech Rock Eng* 49(8):3243–3256
- Feng XX, Jiang QH, Zhang XB, Zhang HC (2018) Shaking table model test on the dynamic response of anti-dip rock slope. *Geotech Geol Eng*:1–11
- Gorum T, Fan XM, Westen CJ, Huang RQ, Xu Q, Tang C, Wang GH (2011) Distribution pattern of earthquake-induced landslides triggered by the 12 May 2008 Wenchuan earthquake. *Geomorphology* 133:152–167
- Guo Z, Wang G, Wang SM (2017) Analysis of landslide stability of the Three Gorges Reservoir bank collapse. *Shanxi Architecture* 43(3): 44–46
- He KQ, Yang JB, Wang SJ (2007) Displacement dynamic theory of accumulation landslide and its application - a case study of typical accumulation landslide in Three Gorges Reservoir Area. Science Press, Beijing
- He JM, Li X, Li SD, Yin YP, Qian HT (2010) Study of seismic response of colluvium accumulation slope by particle flow code. *Granul Matter* 12(5):483–490
- Hu XL, Zhang M, Sun MJ, Huang KX, Song YJ (2015) Deformation characteristics and failure mode of the Zhujiadian landslide in the Three Gorges Reservoir, China. *Bull Eng Geol Environ* 74(1):1–12
- Huang RQ, Li WL (2009) Development and distribution of geohazards triggered by the 5.12 Wenchuan Earthquake in China. *Sci China, Ser E: Technol Sci* 52(4):810–819
- Huang ZQ, Law KT, Liu HD, Jiang T (2009) The chaotic characteristics of landslide evolution: a case study of Xintan landslide. *Environ Geol* 56(8):1585–1591
- Huang BL, Yin YP, Liu GN, Wang SC, Chen XT, Huo ZT (2012) Analysis of waves generated by Gongjiafang landslide in Wu Gorge, three Gorges reservoir, on November 23, 2008. *Landslides* 9:395–405
- Jia XM, Chai HJ, Zheng YR (2010) Mesomechanics research of large direct shear test on soil and rock aggregate mixture with particle flow code simulation. *Rock Soil Mech* 31(9):2695–2703
- Jiang J (2012a) Research on the deformation mechanism and dynamic response of typical landslides in Three Gorges Reservoir in case of frequent microseisms. Dissertation. China University of Geosciences 27(3):624–632
- Jiang JW (2012b) Research on the deformation mechanism and dynamic response of typical landslides in Three Gorges Reservoir in case of frequent microseisms. Wuhan: China University of Geosciences, Wuhan
- Li YJ, Huang GL (2008) Two points of understanding of reservoir induced earthquakes. *Technology for Earthquake Disaster Prevention* 3(1):61–71
- Li CR, Wang M, Liu K, Xie J (2018) Topographic changes and their driving factors after 2008 Wenchuan earthquake. *Geomorphology* 311:27–36
- Liu XR, Fu Y, Wang YX, Huang LY, Qin XY (2009) Stability of reservoir bank slope under water-rock interaction. *Rock Soil Mech* 30(3): 613–616
- Liu XR, Fu Y, Zheng YR, Liang LH (2012a) A review on deterioration of rock caused by water-rock interaction. *Chinese Journal of Underground Space and Engineering* 8(1):77–82
- Liu HX, Xu Q, Fan XM, Xu HB (2012b) Influence of ground motion intensity on dynamic response laws of slope accelerations. *Rock Soil Mech* 33(5):1357–1365
- Liu XR, He CM, Liu SL, Liu YQ, Lu YM, Liu ZH (2018) Dynamic response and failure mode of slopes with horizontal soft and hard interbeddings under frequent microseisms. *Arab J Sci Eng* 43(10): 5397–5411
- Massey C, Della PF, Holden C, Kaiser A, Richards L, Wartman J, McSaveney MJ, Archibald G, Yetton M, Janku L (2017) Rock slope response to strong earthquake shaking. *Landslides* 14(1):249–268
- Shu ZL, Liu BX, Liang NH (2012) Study on the fractal characteristics of earth-rock coarse grain based on digital image processing. *Chinese Journal of Underground Space and Engineering* 8(3):511–516
- Srilatha N, Madhavi LG, Puttappa CG (2013) Effect of frequency on seismic response of reinforced soil slopes in shaking table tests. *Geotext Geomembr* 36:27–32
- Suzanne P (2003) Balancing environment and development. *International water power & dam construction* 3:34–38
- Tang LS (2013) Research on stability and prediction for the colluvial landslide in the Three Gorges Reservoir. China University of Geosciences, Wuhan, Wuhan
- Tang HM, Liu X, Hu XL, Griffiths DV (2015) Evaluation of landslide mechanisms characterized by high-speed mass ejection and long-

- run-out based on events following the Wenchuan earthquake. *Eng Geol* 194:12–24
- Tanoli JJ, Ningsheng C, Regmi AD, Jun L (2017) Spatial distribution analysis and susceptibility mapping of landslides triggered before and after Mw7.8 Gorkha earthquake along Upper Bhote Koshi, Nepal. *Arabian Journal of Geosciences* 10: 277
- Tao ZP (2006) Basic characteristics of reservoir induced earthquakes and engineering preventive measures. *Yunnan Water Power* 22(4): 19–21
- Tao TJ, Chi EA, Zhao MS, Kang Q (2014) Stability analysis of soil slope under strong earthquake. *Applied Mechanics and Materials* (602-605), 598-601
- Wang RS (2004) Fighting the floods. *International water power & dam construction* 2:14–16
- Wang KL, Lin ML (2011) Initiation and displacement of landslide induced by earthquake - a study of shaking table model slope test. *Eng Geol* 122(1–2):106–114
- Wang FW, Zhang YM, Huo ZT, Peng XM, Araiba K, Wang GH (2008) Movement of the Shuping landslide in the first four years after the initial impoundment of the Three Gorges Dam Reservoir China. *Landslides* 5(3):321–329
- Wang M, Liu M, Yang S, Shi P (2014) Incorporating triggering and environmental factors in the analysis of earthquake-induced landslide hazards. *Int J Disaster Risk Sci* 5(2):125–135
- Wang NT, Shi TT, Peng K, Zhang W, Jin XW (2015) Assessment of geohazard susceptibility based on RS and GIS analysis in Jianshi County of the Three Gorges Reservoir, China. *Arab J Geosci* 8: 67–86
- Wartman J, Seed RB, Bray JD (2005) Shaking table modeling of seismically induced deformations in slopes. *J Geotech Geoenviron* 131(5): 610–622
- Wu FF, Cao P, Wan LH (2007) Similarity theory and its application in simulation test. *Min Technol* 4:64–65
- Xu GX, Yao LK, Gao ZN, Li CH (2008) Large-scale shaking table model test study on dynamic characteristics and dynamic responses of slope. *Chin J Rock Mech Eng* 27(3):624–632
- Yang J, Li JB, Lin G (2005) A simple approach to integration of acceleration data for dynamic soil–structure interaction analysis. *Soil Dyn Earthq Eng* 26(8)
- Yang CW, Zhang JJ, Zhou DP (2013) Research on time-frequency analysis method for seismic stability of rock slope subjected to sv wave. *Chin J Rock Mech Eng* 32(3):483–491
- Ye HL, Zheng YR, Li AH, Du XL (2012) Shaking table tests on stabilizing piles of slopes under earthquakes. *Chinese Journal of Geotechnical Engineering* 2:251–257
- Yin Y (2008) Researches on the geo-hazards triggered by Wenchuan Earthquake, Sichuan. *J Eng Geol* 16(4):433–444
- Zhang F, Li JR, Yang L (2012) Accumulation zone landslides deformation feature of Shaxi town in Three Gorges Reservoir area. *J of China Three Gorges Univ (Natural Sciences)* 34(6):48–52
- Zhang JQ, Gurung DR, Liu RQ, Murthy MSR, Su FH (2015) Abe Berek landslide and landslide susceptibility assessment in Badakhshan Province, Afghanistan. *Landslides* 12(3):597–609
- Zhao P (2009) Study on the reservoir induced seismicity in Chongqing under the running of the Three Gorges Reservoir. Chongqing Jiaotong University, Chongqing
- Zhou Z, Wang HG, Fu HL, Liu BC (2009) Influences of rainfall infiltration on stability of accumulation slope by in-situ monitoring test. *J Cent South Univ* 16(2):297–302
- Zhou J, Cui P, Yang X (2013) Dynamic process analysis for the initiation and movement of the Donghekou landslide-debris flow triggered by the Wenchuan earthquake. *J Asian Earth Sci* 76:70–84